

# On the possible noble gas deficiency of Pluto's atmosphere

Olivier Mosis

*Université de Franche-Comté, Institut UTINAM, CNRS/INSU, UMR 6213, Besançon  
Cedex, France*

*Université de Toulouse; UPS-OMP; CNRS-INSU; IRAP; 14 Avenue Edouard Belin,  
31400 Toulouse, France*

Jonathan I. Lunine

*Center for Radiophysics and Space Research, Space Sciences Building Cornell  
University, Ithaca, NY 14853, USA*

Kathleen E. Mandt

*Space Science and Engineering Division, Southwest Research Institute, San Antonio, TX  
78228, USA*

Rebecca Schindhelm

*Southwest Research Institute, 1050 Walnut Street, Boulder, CO 8030223, USA*

Harold A. Weaver

*Space Department, Johns Hopkins University Applied Physics Laboratory, 11100 Johns  
Hopkins Road, Laurel, MD 20723-6099, USA*

S. Alan Stern

*Southwest Research Institute, 1050 Walnut Street, Boulder, CO 8030223, USA*

J. Hunter Waite

*Space Science and Engineering Division, Southwest Research Institute, San Antonio, TX  
78228, USA*

Randy Gladstone

*Space Science and Engineering Division, Southwest Research Institute, San Antonio, TX  
78228, USA*

---

*Email address: [olivier.mosis@obs-besancon.fr](mailto:olivier.mosis@obs-besancon.fr) (Olivier Mosis)*

Audrey Moudens

*LERMA, Université de Cergy-Pontoise, Observatoire de Paris, ENS, UPMC, UMR 8112  
du CNRS, 5 mail Gay Lussac, 95000 Cergy Pontoise Cedex, France*

---

**Abstract**

We use a statistical-thermodynamic model to investigate the formation and composition of noble-gas-rich clathrates on Pluto's surface. By considering an atmospheric composition close to that of today's Pluto and a broad range of surface pressures, we find that Ar, Kr and Xe can be efficiently trapped in clathrates if they formed at the surface, in a way similar to what has been proposed for Titan. The formation on Pluto of clathrates rich in noble gases could then induce a strong decrease in their atmospheric abundances relative to their initial values. A clathrate thickness of order of a few centimeters globally averaged on the planet is enough to trap all Ar, Kr and Xe if these noble gases were in protosolar proportions in Pluto's early atmosphere. Because atmospheric escape over an extended period of time (millions of years) should lead to a noble gas abundance that either remains constant or increases with time, we find that a potential depletion of Ar, Kr and Xe in the atmosphere would best be explained by their trapping in clathrates. A key observational test is the measurement of Ar since the Alice UV spectrometer aboard the New Horizons spacecraft will be sensitive enough to detect its abundance  $\sim 10$  times smaller than in the case considered here.

*Keywords:* Pluto, surface – Pluto, atmosphere – Ices – Triton –  
Trans-neptunian objects

---

## 1. Introduction

Gas hydrates, or clathrates, may exist throughout the solar system. Comparison of predicted stability fields of clathrates with conditions in various planetary environments suggest that these structures could be present in the Martian permafrost (Musselwhite & Lunine 1995; Thomas et al. 2009; Swindle et al. 2009; Herri & Chassefière 2012; Mousis et al. 2013), on the surface and in the interior of Titan (Tobie et al. 2006; Mousis & Schmitt 2008), and in other icy satellites (Prieto-Ballesteros et al. 2005; Hand et al. 2006). It has also been suggested that the activity of many comets could result from the destabilization of these ices (Marboeuf et al. 2010, 2011, 2012a). On Earth, the destabilization of significant masses of  $\text{CO}_2$  and  $\text{CH}_4$  potentially stored in clathrates buried in seabeds and permafrost is regarded as a possible aggravating factor in future global warming (clathrate gun hypothesis – Kennett et al. 2003). Broadly speaking, clathrates are thought to have taken part in the assemblage of the building blocks of many bodies of the solar system and may be in other planetary systems (Lunine & Stevenson 1985; Mousis et al. 2002, 2006, 2009, 2010, 2011, 2012a; Mousis & Gautier 2004; Alibert et al. 2005; Marboeuf et al. 2008; Madhusudhan et al. 2011; Johnson et al. 2012).

Clathrates have also been proposed to be at the origin of the noble gas deficiency measured in situ by the Huygens probe in the atmosphere of Titan (Osegovic & Max 2005; Thomas et al. 2007, 2008; Mousis et al. 2011). In the case of Mars, important quantities of argon, krypton and xenon are believed to be trapped in clathrates located in the near subsurface and their storage in these structures could explain the measured two order of magni-

26 tude drop between the noble gas atmospheric abundances in Earth and Mars  
 27 (Mousis et al. 2012b). Here we investigate the possibility of formation of  
 28 clathrates rich in noble gases on Pluto’s surface. To do so, we use the same  
 29 statistical-thermodynamic model applied to the case of Titan to determine  
 30 the composition of clathrates that might form on Pluto and to investigate  
 31 the possible consequences of their presence on the atmospheric composition.

## 32 **2. The statistical–thermodynamic model**

33 To calculate the relative abundances of guest species incorporated in a  
 34 multiple guest clathrate (hereafter MG clathrate) at given temperature and  
 35 pressure, we use a model applying classical statistical mechanics that relates  
 36 the macroscopic thermodynamic properties of clathrates to the molecular  
 37 structure and interaction energies (van der Waals & Platteuw 1959; Lu-  
 38 nine & Stevenson 1985). It is based on the original ideas of van der Waals  
 39 and Platteuw for clathrate formation, which assume that trapping of guest  
 40 molecules into cages corresponds to the three-dimensional generalization of  
 41 ideal localized adsorption.

42 In this formalism, the fractional occupancy of a guest molecule  $K$  for a  
 43 given type  $t$  ( $t = \text{small or large}$ ) of cage (see Sloan 1998; Sloan & Kohn 2008)  
 44 can be written as

$$y_{K,t} = \frac{C_{K,t}P_K}{1 + \sum_J C_{J,t}P_J}, \quad (1)$$

45 where the sum in the denominator includes all the species which are present  
 46 in the initial gas phase.  $C_{K,t}$  is the Langmuir constant of species  $K$  in the  
 47 cage of type  $t$ , and  $P_K$  is the partial pressure of species  $K$ . This partial

48 pressure is given by  $P_K = x_K \times P$  (we assume that the sample behaves  
 49 as an ideal gas), with  $x_K$  the mole fraction of species  $K$  in the initial gas,  
 50 and  $P$  the total atmospheric gas pressure, which is dominated by  $N_2$ . The  
 51 Langmuir constant depends on the strength of the interaction between each  
 52 guest species and each type of cage, and can be determined by integrating  
 53 the molecular potential within the cavity as

$$C_{K,t} = \frac{4\pi}{k_B T} \int_0^{R_c} \exp\left(-\frac{w_{K,t}(r)}{k_B T}\right) r^2 dr, \quad (2)$$

54 where  $R_c$  represents the radius of the cavity assumed to be spherical,  $k_B$  the  
 55 Boltzmann constant, and  $w_{K,t}(r)$  is the spherically averaged Kihara potential  
 56 representing the interactions between the guest molecules  $K$  and the  $H_2O$   
 57 molecules forming the surrounding cage  $t$ . This potential  $w(r)$  can be written  
 58 for a spherical guest molecule, as (McKoy & Sinanoğlu 1963)

$$w(r) = 2z\epsilon \left[ \frac{\sigma^{12}}{R_c^{11}r} \left( \delta^{10}(r) + \frac{a}{R_c} \delta^{11}(r) \right) - \frac{\sigma^6}{R_c^5 r} \left( \delta^4(r) + \frac{a}{R_c} \delta^5(r) \right) \right], \quad (3)$$

59 with

$$\delta^N(r) = \frac{1}{N} \left[ \left( 1 - \frac{r}{R_c} - \frac{a}{R_c} \right)^{-N} - \left( 1 + \frac{r}{R_c} - \frac{a}{R_c} \right)^{-N} \right]. \quad (4)$$

60 In Eq. 3,  $z$  is the coordination number of the cell. This parameter depends  
 61 on the structure of the clathrate (I or II; see Sloan & Koh 2008) and on the  
 62 type of the cage (small or large). The Kihara parameters  $a$ ,  $\sigma$  and  $\epsilon$  for the  
 63 molecule-water interactions, given in Table A.1, have been taken from the

64 recent compilation of Sloan & Koh (2008) when available and from Parrish  
 65 & Prausnitz (1972) for the remaining species.

66 Finally, the mole fraction  $f_K$  of a guest molecule  $K$  in a clathrate can be  
 67 calculated with respect to the whole set of species considered in the system  
 68 as

$$f_K = \frac{b_s y_{K,s} + b_l y_{K,l}}{b_s \sum_J y_{J,s} + b_l \sum_J y_{J,l}}, \quad (5)$$

69 where  $b_s$  and  $b_l$  are the number of small and large cages per unit cell respec-  
 70 tively, for the clathrate structure under consideration, and with  $\sum_K f_K = 1$ .  
 71 Values of  $R_c$ ,  $z$ ,  $b_s$  and  $b_l$  are taken from Parrish & Prausnitz (1972).

72 In the present approach, the dissociation pressure of the MG clathrate  
 73 and the mole fractions of the trapped volatiles are independently calculated.  
 74 All mole fraction calculations are performed at the dissociation pressure  $P =$   
 75  $P_{mix}^{diss}$  of the clathrate, i.e. temperature and pressure conditions at which this  
 76 ice forms. This dissociation pressure can be deduced from the dissociation  
 77 pressure  $P_K^{diss}$  of a pure clathrate of species  $K$ , as (Hand et al. 2006; Thomas  
 78 et al. 2007):

$$P_{mix}^{diss} = \left( \sum_K \frac{x_K}{P_K^{diss}} \right)^{-1}, \quad (6)$$

79 where  $x_K$  is the atmospheric mole fraction of species  $K$  and  $P_K^{diss}$  its disso-  
 80 ciation pressure.  $P_K^{diss}$  derives from laboratory measurements and follows an  
 81 Arrhenius law (Miller 1961) as

$$\log(P^{diss}) = A + \frac{B}{T}, \quad (7)$$

82 where  $P^{\text{diss}}$  is expressed in Pa and  $T$  is the temperature in K. The constants  
83  $A$  and  $B$  for  $\text{N}_2$  and Ar have been fitted to experimental data (Lunine &  
84 Stevenson 1985; Sloan 1998) and those for Xe and Kr have been taken from  
85 Fray et al. (2010) and Marboeuf et al. (2012b), respectively (see Table A.2).

### 86 **3. Clathrate production on Pluto**

87 Depending on its composition, the dissociation pressure of MG clathrate  
88 varies between  $\sim 5.1 \times 10^{-10}$  and  $2.1 \times 10^{-5}$  Pa at Pluto's average surface  
89 temperature ( $\sim 50$  K; Lellouch et al. 2000), a value well below the atmo-  
90 spheric surface pressure which lies in the 0.65–2.4 Pa range (Elliot et al.  
91 2003; Sicardy et al. 2003). This implies that MG clathrate remains stable  
92 at the surface irrespective of Pluto's seasonal variations and that its dissoci-  
93 ation and reformation cannot occur under the planet's current atmospheric  
94 conditions. The only conditions on Pluto's surface allowing MG clathrate  
95 formation from an initial inventory present in the atmosphere require that  
96 the surface be hotter than the present-day temperature, most likely at early  
97 epochs after the planet's formation (see e.g. Fig. 1 of McKinnon 2002) or  
98 during the collisions that engendered the Pluto–Charon binary system (McK-  
99 innon 1988, 1989). An alternative possibility would be the recent or ancient  
100 release of hot ice from the interior of Pluto as the result of cryovolcanic  
101 events (Cook et al. 2007). It is during clathrate formation that substantial  
102 amounts of volatiles might have been sequestered from the atmosphere into  
103 the surface.

104 Table A.3 gives the composition of Pluto's proto-atmosphere used in our  
105 calculations. We made the conservative assumption that all noble gases were

106 initially present in the proto-atmosphere of Pluto, with Ar/N, Kr/N and  
107 Xe/N ratios assigned to be protosolar (Asplund et al. 2009). Because Pluto’s  
108 proto-atmosphere is expected to be strongly dominated by N<sub>2</sub> and that N<sub>2</sub>  
109 clathrate is of structure II (Lunine & Stevenson 1985; Sloan & Koh 2008),  
110 we show here calculations of the MG clathrate composition only for this  
111 structure. It is also important to note that our composition calculations are  
112 only valid along the dissociation curve of the clathrate of interest (see Fig.  
113 A.1).

114 From our calculations, we find that three kinds of clathrates with distinct  
115 compositions might form on Pluto’s surface, each of them containing noble  
116 gases in different proportions. Figure A.2 shows the composition of these  
117 clathrates computed for an atmospheric pressure ranging between 1 and 10<sup>3</sup>  
118 Pa. Note that these surface pressures correspond to a MG clathrate equi-  
119 librium temperature in the ~80–100 K range. If a greater surface pressure  
120 is considered, then the MG clathrate will also form at a higher equilibrium  
121 temperature. A first layer forms from the gas phase composition depicted in  
122 Table A.3. Irrespective of the pressure considered, the mole fraction of Xe  
123 trapped in this clathrate is between ~0.15 and 0.76, i.e. a range of values  
124 that is ~31,000–159,000 times larger than its atmospheric mole fraction. The  
125 mole fraction of Kr is also substantially enhanced by a factor of ~400–750 in  
126 clathrate compared to its atmospheric value. In contrast, the mole fraction  
127 of Ar trapped in clathrate evolves from a slight impoverishment (~0.5) to a  
128 moderate enrichment (~3) with increasing pressure, compared to its atmo-  
129 spheric value. The second clathrate layer forms once Xe is fully trapped in  
130 the first layer. In this case, only N<sub>2</sub>, Kr and Ar remain in the gas phase (the



131 mole fractions of these species trapped in the first layer remain negligible).  
132 The mole fraction of Kr trapped in this clathrate is enhanced by a factor  
133 of 400–4,000 times compared to its atmospheric mole fraction in the 1–10<sup>3</sup>  
134 Pa pressure range. The Ar mole fraction in this layer is also found to be  
135 moderately enriched by a factor of  $\sim 2$ –3, compared to its atmospheric mole  
136 fraction. In its turn, a third clathrate layer forms when Kr is fully trapped  
137 in the second layer and in this case only N<sub>2</sub> and Ar remain in the coexisting  
138 gas phase. The fraction of Ar trapped in this clathrate remains constant  
139 irrespective of the surface pressure considered and is found to be  $\sim 3$  times  
140 larger than its atmospheric value.

141 If Ar, Kr and Xe were initially in protosolar abundances in the atmosphere  
142 of Pluto, the amount of clathrates needed for their sequestration is relatively  
143 low. For example, if the three clathrate layers formed at their equilibrium  
144 temperatures<sup>1</sup> for a surface pressure of 2.4 Pa, their total equivalent thickness  
145 is of order  $\sim 4$  mm globally averaged on the planet, assuming a full clathration  
146 efficiency and the presence of a structure II clathrate. Interestingly, calcula-  
147 tions conducted in the case of formation of structure I clathrate lead to similar  
148 conclusions. The noble gas trapping efficiencies are still very high but require  
149 an overall thickness of the three clathrate layers of  $\sim 2$  cm. In both clathrate  
150 structures, the equivalent layer of the Ar-dominated clathrate is more than 3  
151 orders of magnitude thicker than those of Xe- and Kr-dominated clathrates.  
152 One must also note that the noble-gas-rich clathrates formed on Pluto could  
153 consist in a mixture of structures I and II clathrates. Indeed, in our com-

---

<sup>1</sup>The equilibrium temperatures of the first, second and third clathrate layers are  $\sim 77$ ,  
76 and 76 K, respectively.

154 putations of the composition of structure II clathrates, we find that the first  
 155 layer formed is dominated by Xe, which is itself predicted to form a structure  
 156 I clathrate (Sloan & Koh 2008).

#### 157 4. Competition with atmospheric escape

158 An alternative method for losing these noble gases from Pluto’s atmo-  
 159 sphere could be atmospheric escape. The atmosphere of Pluto is expected to  
 160 escape efficiently due to Pluto’s low gravity (Strobel 2008), though debate  
 161 exists as to whether the escape rate is greater than subsonic (Tucker et al.  
 162 2012). If the escape of Pluto’s atmosphere is hydrodynamic (Trafton et al.  
 163 1997; Strobel 2008), the outflow of N<sub>2</sub> provides enough energy to drag Ar,  
 164 Kr and Xe from the atmosphere. The escape rate of these gases depends  
 165 directly on the escape rate of N<sub>2</sub> (Hunten et al. 1987):

$$F_i = \frac{X_i}{X_{N_2}} F_{N_2} \left( \frac{m_c - m_i}{m_c - m_{N_2}} \right), \quad (8)$$

166 where  $F$  is the escape flux,  $X$  is the abundance of the noble gas (subscript  $i$ )  
 167 and N<sub>2</sub>,  $m$  is the mass of each constituent and  $m_c$  is the critical mass which  
 168 is also a function of the N<sub>2</sub> escape rate (Hunten et al. 1987):

$$m_c = m_{N_2} + \frac{k T F_{N_2}}{b g X_{N_2}}, \quad (9)$$

169 where  $k$  is the Boltzmann’s constant,  $T$  is the temperature,  $b$  is the binary  
 170 diffusion coefficient given as  $b = AT^s$  with  $A$  and  $s$  constants determined  
 171 through modeling or laboratory measurements, and  $g$  is the acceleration due  
 172 to gravity.

173 It is clear from Eq. 9 that the critical mass is always greater than the  
174 mass of  $N_2$ , so constituents with mass less than  $N_2$  are always subject to  
175 escape when hydrodynamic escape is occurring. Ar, Kr and Xe all have  
176 masses greater than  $N_2$ , but the proposed escape rate of  $N_2$  is so high that  
177 the critical mass is several times greater than the mass of Xe and the last term  
178 in Eq. 8 has a value of 1.0. This means that the escape rate of the noble gases  
179 relative to the escape rate of  $N_2$ , under hydrodynamic escape conditions, is  
180 equivalent to the abundance of the noble gas relative to  $N_2$  as suggested in  
181 Eq. 8. Therefore, at the highest possible escape rate for the noble gases,  
182 the abundance of the noble gas relative to  $N_2$  will remain constant. In the  
183 case of escape rates that are subsonic, escape of the noble gases will be far  
184 less efficient due to insufficient energy to drag the heavier molecules from  
185 the atmosphere. As a result, the noble gas escape rate relative to  $N_2$ 's rate  
186 of escape will be less than the abundance of the noble gases relative to  $N_2$   
187 in the atmosphere. Over time, the differential escape rates will lead to an  
188 increase in the noble gas abundance in Pluto's atmosphere. This means that  
189 without trapping of Ar by clathrates, escape over an extended period of time  
190 (millions of years) will lead to a noble gas abundance that either remains  
191 constant or increases with time. Therefore, a depletion of Ar, Kr and Xe  
192 in the atmosphere can best be explained by trapping of the noble gases in  
193 clathrates.

## 194 5. Discussion

195 Using the noble gas abundances given in Table A.3 and the fitting laws  
196 of sublimation laboratory data proposed by Fray & Schmitt (2009), we find

197 that the equilibrium temperatures of Ar, Kr and Xe pure ices are  $\sim 39.5$ ,  
198 42.5 and 55.3 K at the surface pressure of 2.4 Pa, respectively. Given Pluto's  
199 average surface temperature ( $\sim 50$  K), Xe appears stable on the surface in  
200 present-day conditions and the condensation of this noble gas should also  
201 induce a decrease of its atmospheric abundance. This implies that there is  
202 no way to disentangle Xe's previous trapping in clathrate versus its simple  
203 condensation. This is fortunately not the case for Ar and Kr, so the mea-  
204 surement of at least one of these two noble gases is critical for testing the  
205 scenario of clathrate trapping. The UV spectrometer Alice aboard the New  
206 Horizons spacecraft will be sensitive enough to detect an argon abundance  
207 that is  $\sim 10$  times smaller than protosolar Ar/N in some circumstances (see  
208 appendix Appendix A).

209 Our scenario of the noble gas trapping in clathrates on Pluto is motivated  
210 by the fact that the same interpretation was provided in the case of Titan  
211 in order to account for its observed noble gas deficiency (Osegovic & Max  
212 2005; Thomas et al. 2007, 2008; Mousis et al. 2011). The situation here  
213 is much more favorable than in the case of Titan since the clathrate layer  
214 required on Pluto's surface is  $\sim 10^4$  times thinner. This is essentially due to  
215 the difference between the surface pressures since the two atmospheres are  
216 both dominated by  $N_2$ .

217 Note that our model considers only the trapping of the noble gases that  
218 were present in the early atmosphere. It does not exclude the possibility  
219 that the bulk of these noble gases is still in the interior of Pluto. However,  
220 if there is outgassing, the noble gases released in the atmosphere should be  
221 trapped as well by clathrates. Our calculations are also valid irrespective of

222 the source (primordial or radiogenic) of the noble gases potentially present  
223 in Pluto's atmosphere. Indeed, since Pluto is  $\sim$ half rock, a significant part  
224 of the existing argon could result from the radiogenic decay of potassium-40.

225 Interestingly, similar calculations have been performed in the case of Tri-  
226 ton and they lead to conclusions as favorable as in the case of Pluto. However,  
227 the surface temperature of Triton,  $\sim$ 38 K (Tryka et al. 1994), is much lower  
228 than Pluto's. It is low enough that the condensation of the three noble gases  
229 as pure ices on the surface would largely remove them from the atmosphere  
230 irrespective of their sequestration in clathrate. Nonetheless, a mass spec-  
231 trometer directly sampling Triton's atmosphere could in principle detect the  
232 atmospheric abundances of all three noble gases to assess if they were con-  
233 sistent with coexistent surface ices. Since the atmospheric abundances in  
234 coexistence with crustal clathrate are orders of magnitude smaller (probably  
235 too small for detection), this provides an eventual test of the hypothesis in  
236 the case of a future mission to the Neptune system.

## 237 **6. Conclusions**

238 By considering an atmospheric composition close to that of today's Pluto  
239 and a broad range of surface pressures, we find that Ar, Kr and Xe can be  
240 efficiently trapped in clathrates if they formed at the surface. The formation  
241 of noble gas-rich clathrates on Pluto could then induce a strong decrease of  
242 their initial atmospheric abundances. A clathrate thickness of order of a few  
243 centimeters globally averaged on the planet is indeed enough to trap Ar, Kr  
244 and Xe irrespective of the clathrate structure, if they were in protosolar pro-  
245 portions in the early Pluto's atmosphere. We suggest that the measurement

246 of the Ar abundance by the Alice ultraviolet spectrometer (Stern et al. 2008)  
247 aboard the New Horizons spacecraft during Pluto’s flyby should provide a  
248 test of the validity of our scenario.

## 249 **Acknowledgements**

250 O. Mousis acknowledges support from CNES. J.I. Lunine was supported  
251 by a contract from JPL under the Distinguished Visiting Scientist program.  
252 J. H. Waite acknowledges support from NASA Rosetta funding.

## 253 **Appendix A. Estimating Argon Airglow Emission for the New** 254 **Horizons Mission**

255 With the nominal Pluto encounter of the New Horizons mission fully  
256 planned, we wish to estimate the amount of Ar I that can be detected by the  
257 Alice UVS instrument during approach. There will be 11 Alice observations  
258 at close range on approach dedicated to measuring extended airglow emission,  
259 with integrations times ranging from 360 to 6900 seconds each, for a total of  
260 approximately 6 hours of integration. The midpoint distances from Pluto for  
261 these observations range from  $1 \times 10^6$  km to  $3 \times 10^5$  km. We use the planned  
262 observation times and their corresponding midpoint distances, as well as the  
263 Alice effective area at the Ar I doublet (104.8, 106.7 nm), to estimate the  
264 signal to noise ratio (SNR) for a given Ar I mixing ratio.

265 The Ar I brightness was determined using the Atmospheric Ultraviolet  
266 Radiance Integrated Code (hereafter AURIC) (Strickland et al. 1999). This  
267 was run with Ar I abundances of 0.1%, 0.3%, 1%, 3%, and 10%, to pro-  
268 duce volume production rates from photoelectron impact and photoexcita-

269 tion processes. “Model 2” densities from Krasnopolsky & Cruikshank (1999)  
 270 were used for N<sub>2</sub> and CH<sub>4</sub> in the model atmosphere ( $7.1 \times 10^{13} \text{ cm}^{-3}$  and  
 271  $6.4 \times 10^{11} \text{ cm}^{-3}$ , respectively), with laboratory measured cross sections and  
 272 TIMED/SEE solar spectral irradiance for excitation. The Ar I brightnesses  
 273 fed into the Alice UVS model thus are the emergent intensities upwelling  
 274 through the N<sub>2</sub>/CH<sub>4</sub> atmosphere to space.

275 Figure A.3 shows simulated brightness images for one of the approach  
 276 observations, along with the observation coordinates. Figure A.4 shows the  
 277 curve of growth made with the brightness estimates for each Ar I abundance  
 278 simulated. We use this brightness relation to calculate the SNR obtained with  
 279 the Alice airglow observations. The total counts obtained ( $C$  in photons) in  
 280 the Alice slit is just:

$$C = \frac{10^6}{4\pi} R A \sum t_i \Omega_i \quad (\text{A.1})$$

281 where  $R$  is the brightness (Rayleighs), and  $A$  is the effective area ( $0.1 \text{ cm}^2$  at  
 282 the Ar I doublet). Since each observation differs in length ( $t_i$  in seconds) and  
 283 is performed at different distances (leading to different solid angles), we sum  
 284 the photons piecewise.  $\Omega_i$  is the effective solid angle of the emitting object  
 285 visible in the slit. The different exposure times ( $t_i$ ), midpoint distances from  
 286 Pluto ( $d_i$ ), and slit-filling solid angle for each observation are listed in Table  
 287 A.4.

288 For our SNR estimates we consider only the emission from the area of  
 289 Pluto’s solid disk. We assume a detector background dark rate of 0.02 counts  
 290 per spatial/spectral element (as measured in flight) and the AURIC bright-  
 291 ness estimates of the 104.8 and 106.7 nm Ar I emission lines to calculate the

292 SNR for a given mixing ratio, shown in Figure A.5.

293 With these calculations we conclude that in 6 hours of observing on final  
294 approach to Pluto, the Alice instrument should be able to detect Argon emis-  
295 sion in Pluto's atmosphere even at lower than solar abundances. Assuming a  
296 number abundance of 0.25 ppm for Ar I and 36 ppm for N<sub>2</sub>, i.e., at one tenth  
297 solar abundance, the SNR will be ~16. Unfortunately, the measurements of  
298 Kr and Xe abundances in the atmosphere of Pluto is beyond the instrument's  
299 capabilities.

## 300 **References**

- 301 [1] Alibert, Y., Mousis, O., Benz, W. 2005. On the Volatile Enrichments  
302 and Composition of Jupiter. *The Astrophysical Journal* 622, L145-L148.
- 303 [2] Asplund, M., Grevesse, N., Sauval, A. J., Scott, P. 2009. The Chemical  
304 Composition of the Sun. *Annual Review of Astronomy and Astrophysics*  
305 47, 481-522.
- 306 [3] Cook, J. C., Desch, S. J., Roush, T. L., Trujillo, C. A., Geballe, T. R.  
307 2007. Near-Infrared Spectroscopy of Charon: Possible Evidence for Cry-  
308ovolcanism on Kuiper Belt Objects. *The Astrophysical Journal* 663,  
309 1406-1419.
- 310 [4] Elliot, J. L., and 28 colleagues 2003. The recent expansion of Pluto's  
311 atmosphere. *Nature* 424, 165-168.
- 312 [5] Fray, N., Marboeuf, U., Brissaud, O., Schmitt, B.. 2010. Equilibrium  
313 data of methane, carbon dioxide, and xenon clathrate hydrates below



- 314 the freezing point of water. *Applications to Astrophysical Environments.*  
315 *Journal of Chemical & Engineering* 55, 5101-5208.
- 316 [6] Fray, N., Schmitt, B. 2009. Sublimation of ices of astrophysical interest:  
317 A bibliographic review. *Planetary and Space Science* 57, 2053-2080.
- 318 [7] Hand, D. P., Chyba, C. F., Carlson, R. W., Cooper, J. F. 2006. Clathrate  
319 Hydrates of Oxidants in the Ice Shell of Europa. *Astrobiology* 6, 463-482.
- 320 [8] Herri, J.-M., Chassefière, E. 2012. Carbon dioxide, argon, nitrogen and  
321 methane clathrate hydrates: Thermodynamic modelling, investigation  
322 of their stability in Martian atmospheric conditions and variability of  
323 methane trapping. *Planetary and Space Science* 73, 376-386.
- 324 [9] Hunten, D. M., Pepin, R. O., Walker, J. C. G. 1987. Mass fractionation  
325 in hydrodynamic escape. *Icarus* 69, 532-549.
- 326 [10] Kennett, J. P., Cannariato, K. G., Hendy, I. L., Behl, R. J. 2003.  
327 Methane Hydrates in Quaternary Climate Change: The Clathrate Gun  
328 Hypothesis, 216 pp., AGU, Washington, D. C., doi:10.1029/054SP.
- 329 [11] Johnson, T. V., Mousis, O., Lunine, J. I., Madhusudhan, N. 2012. Plan-  
330 etesimal Compositions in Exoplanet Systems. *The Astrophysical Journal*  
331 757, 192.
- 332 [12] Krasnopolsky, V. A., Cruikshank, D. P. 1999. Photochemistry of Pluto's  
333 atmosphere and ionosphere near perihelion. *Journal of Geophysical Re-*  
334 *search* 104, 21979-21996.

- 335 [13] Lellouch, E., Laureijs, R., Schmitt, B., Quirico, E., de Bergh, C., Cro-  
336 visier, J., Coustenis, A. 2000. Pluto's Non-isothermal Surface. *Icarus*  
337 147, 220-250.
- 338 [14] Lunine, J. I., Stevenson, D. J. 1985. Thermodynamics of clathrate hy-  
339 drate at low and high pressures with application to the outer solar sys-  
340 tem. *The Astrophysical Journal Supplement Series* 58, 493-531.
- 341 [15] Madhusudhan, N., Mousis, O., Johnson, T. V., Lunine, J. I. 2011.  
342 Carbon-rich Giant Planets: Atmospheric Chemistry, Thermal Inver-  
343 sions, Spectra, and Formation Conditions. *The Astrophysical Journal*  
344 743, 191.
- 345 [16] Marboeuf, U., Fray, N., Brissaud, O., Schmitt, B., Bockelée-Morvan,  
346 D., Gautier D. 2012b. Equilibrium pressure of ethane, acetylene, and  
347 krypton clathrate hydrates below the freezing point of water. *Journal of*  
348 *Chemical & Engineering* 57, 3408-3415.
- 349 A cometary nucleus model taking into account all phase changes of water  
350 ice: amorphous, crystalline, and clathrate. *Astronomy and Astrophysics*  
351 542, A82.
- 352 [17] Marboeuf, U., Schmitt, B., Petit, J.-M., Mousis, O., Fray, N. 2012a. A  
353 cometary nucleus model taking into account all phase changes of water  
354 ice: amorphous, crystalline, and clathrate. *Astronomy and Astrophysics*  
355 542, A82.
- 356 [18] Marboeuf, U., Mousis, O., Petit, J.-M., Schmitt, B., Cochran, A. L.,  
357 Weaver, H. A. 2011. On the stability of clathrate hydrates in comets

- 358 67P/Churyumov-Gerasimenko and 46P/Wirtanen. *Astronomy and As-*  
359 *trophysics* 525, A144.
- 360 [19] Marboeuf, U., Mousis, O., Petit, J.-M., Schmitt, B. 2010. Clathrate  
361 Hydrates Formation in Short-Period Comets. *The Astrophysical Journal*  
362 708, 812-816.
- 363 [20] Marboeuf, U., Mousis, O., Ehrenreich, D., Alibert, Y., Cassan, A.,  
364 Wakelam, V., Beaulieu, J.-P. 2008. Composition of Ices in Low-Mass  
365 Extrasolar Planets. *The Astrophysical Journal* 681, 1624-1630.
- 366 [21] McKinnon, W. B. 2002. On the initial thermal evolution of Kuiper Belt  
367 objects. *Asteroids, Comets, and Meteors: ACM 2002* 500, 29-38.
- 368 [22] McKinnon, W. B. 1989. On the origin of the Pluto-Charon binary. *The*  
369 *Astrophysical Journal* 344, L41-L44.
- 370 [23] McKinnon, W. B., Mueller, S. 1988. Pluto's structure and composition  
371 suggest origin in the solar, not a planetary, nebula. *Nature* 335, 240-243.
- 372 [24] McKoy, V., Sinanoğlu, O., 1963. Theory of dissociation pressures of  
373 some gas hydrates. *Journal of Chemical Physics* 38 (12), 2946-2956.
- 374 [25] Miller, S. L. 1961. The Occurrence of Gas Hydrates in the Solar System.  
375 *Proceedings of the National Academy of Science* 47, 1798-1808.
- 376 [26] Mousis, O., and 10 colleagues 2013. Volatile Trapping in Martian  
377 Clathrates. *Space Science Reviews*, in press.

- 378 [27] Mousis, O., Lunine, J. I., Chassefière, E., Montmessin, F., Lakhliq, A.,  
379 Picaud, S., Petit, J.-M., Cordier, D. 2012b. Mars cryosphere: A potential  
380 reservoir for heavy noble gases?. *Icarus* 218, 80-87.
- 381 [28] Mousis, O., Lunine, J. I., Madhusudhan, N., Johnson, T. V. 2012a. Neb-  
382 ular Water Depletion as the Cause of Jupiter's Low Oxygen Abundance.  
383 *The Astrophysical Journal* 751, L7.
- 384 [29] Mousis, O., Lunine, J. I., Picaud, S., Cordier, D., Waite, J. H., Jr.,  
385 Mandt, K. E. 2011. Removal of Titan's Atmospheric Noble Gases by  
386 Their Sequestration in Surface Clathrates. *The Astrophysical Journal*  
387 740, L9.
- 388 [30] Mousis, O., Lunine, J. I., Picaud, S., Cordier, D. 2010. Volatile inven-  
389 tories in clathrate hydrates formed in the primordial nebula. *Faraday*  
390 *Discussions* 147, 509.
- 391 [31] Mousis, O., Marboeuf, U., Lunine, J. I., Alibert, Y., Fletcher, L. N.,  
392 Orton, G. S., Pauzat, F., Ellinger, Y. 2009. Determination of the Mini-  
393 mum Masses of Heavy Elements in the Envelopes of Jupiter and Saturn.  
394 *The Astrophysical Journal* 696, 1348-1354.
- 395 [32] Mousis, O., Schmitt, B. 2008. Sequestration of Ethane in the Cryovol-  
396 canic Subsurface of Titan. *The Astrophysical Journal* 677, L67-L70.
- 397 [33] Mousis, O., Alibert, Y., Benz, W. 2006. Saturn's internal structure and  
398 carbon enrichment. *Astronomy and Astrophysics* 449, 411-415.
- 399 [34] Mousis, O., Gautier, D. 2004. Constraints on the presence of volatiles

- 400 in Ganymede and Callisto from an evolutionary turbulent model of the  
401 Jovian subnebula. *Planetary and Space Science* 52, 361-370.
- 402 [35] Mousis, O., Gautier, D., Bockelée-Morvan, D. 2002. An Evolutionary  
403 Turbulent Model of Saturn's Subnebula: Implications for the Origin of  
404 the Atmosphere of Titan. *Icarus* 156, 162-175.
- 405 [36] Musselwhite, D., Lunine, J. I. 1995. Alteration of volatile inventories  
406 by polar clathrate formation on Mars. *Journal of Geophysical Research*  
407 100, 23301-23306.
- 408 [37] Osegovic, J. P., Max, M. D. 2005. Compound clathrate hydrate on Ti-  
409 tan's surface. *Journal of Geophysical Research (Planets)* 110, 8004.
- 410 [38] Parrish, W. R., Prausnitz, J. M., 1972. Dissociation pressures of gas  
411 hydrates formed by gas mixtures. *Industrial and Engineering Chemistry:*  
412 *Process Design and Development*, 11 (1), 26-35. Erratum : Parrish,  
413 W. R., Prausnitz, J. M., 1972. *Industrial and Engineering Chemistry:*  
414 *Process Design and Development* 11 (3), 462.
- 415 [39] Prieto-Ballesteros, O., Kargel, J. S., Fernández-Sampedro, M., Selsis,  
416 F., Martínez, E. S., Hogenboom, D. L. 2005. Evaluation of the possible  
417 presence of clathrate hydrates in Europa's icy shell or seafloor. *Icarus*  
418 177, 491-505.
- 419 [40] Sicardy, B., and 40 colleagues 2003. Large changes in Pluto's atmosphere  
420 as revealed by recent stellar occultations. *Nature* 424, 168-170.
- 421 [41] Sloan, E. D., Koh, C. A., 2008. *Clathrate Hydrates of Natural Gases*.  
422 3rd ed.; CRC Press, Taylor & Francis Group, Boca Raton.

- 423 [42] Sloan, E. D., Jr., 1998. Clathrate hydrates of natural gases. Dekker, M.  
424 (Ed.), New York.
- 425 [43] Stern, S. A., and 10 colleagues 2008. ALICE: The Ultraviolet Imag-  
426 ing Spectrograph Aboard the New Horizons Pluto-Kuiper Belt Mission.  
427 Space Science Reviews 140, 155-187.
- 428 [44] Strickland, D. J., Bishop, J., Evans, J. S., Majeed, T., Shen, P. M.,  
429 Cox, R. J., Link, R., Huffman, R. E. 1999. Atmospheric ultraviolet ra-  
430 diance integrated code (AURIC): theory, software architecture, inputs,  
431 and selected results.. Journal of Quantitative Spectroscopy and Radia-  
432 tive Transfer 62, 689-742.
- 433 [45] Strobel, D. F. 2008. N<sub>2</sub> escape rates from Pluto's atmosphere. Icarus  
434 193, 612-619.
- 435 [46] Swindle, T. D., Thomas, C., Mousis, O., Lunine, J. I., Picaud, S. 2009.  
436 Incorporation of argon, krypton and xenon into clathrates on Mars.  
437 Icarus 203, 66-70.
- 438 [47] Thomas, C., Mousis, O., Picaud, S., Ballenegger, V. 2009. Variability of  
439 the methane trapping in martian subsurface clathrate hydrates. Plane-  
440 tary and Space Science 57, 42-47.
- 441 [48] Thomas, C., Picaud, S., Mousis, O., Ballenegger, V. 2008. A theoretical  
442 investigation into the trapping of noble gases by clathrates on Titan.  
443 Planetary and Space Science 56, 1607-1617.
- 444 [49] Thomas, C., Mousis, O., Ballenegger, V., Picaud, S. 2007. Clathrate

- 445 hydrates as a sink of noble gases in Titan's atmosphere. *Astronomy and*  
446 *Astrophysics* 474, L17-L20.
- 447 [50] Tobie, G., Lunine, J. I., Sotin, C. 2006. Episodic outgassing as the origin  
448 of atmospheric methane on Titan. *Nature* 440, 61-64.
- 449 [51] Trafton, L. M., Hunten, D. M., Zahnle, K. J., McNutt, R. L., Jr. 1997.  
450 Escape Processes at Pluto and Charon. *Pluto and Charon* 475.
- 451 [52] Tryka, K. A., Brown, R. H., Chruikshank, D. P., Owen, T. C., Geballe,  
452 T. R., de Bergh, C. 1994. Temperature of nitrogen ice on Pluto and its  
453 implications for flux measurements. *Icarus* 112, 513-527.
- 454 [53] Tucker, O. J., Erwin, J. T., Deighan, J. I., Volkov, A. N., Johnson, R. E.  
455 2012. Thermally driven escape from Pluto's atmosphere: A combined  
456 fluid/kinetic model. *Icarus* 217, 408-415.
- 457 [54] van der Waals, J. H., Platteeuw, J. C., 1959. Clathrate solutions. In:  
458 *Advances in Chemical Physics*, Vol. 2, Interscience, New York, 1-57.

Table A.1: Parameters for Kihara and Lennard-Jones potentials

Molecule	$\sigma_{K-W}$ (Å)	$\epsilon_{K-W}/k_B$ (K)	$a_{K-W}$ (Å)	Reference
N <sub>2</sub>	3.0993	133.13	0.3526	Herri & Chassefière (2012)
Ar	2.9434	174.14	0.184	Herri & Chassefière (2012)
Kr	2.9739	198.34	0.230	Parrish & Prausnitz (1972)
Xe	3.32968	193.708	0.2357	Sloan & Koh (2008)

$\sigma_{K-W}$  is the Lennard-Jones diameter,  $\epsilon_{K-W}$  is the depth of the potential well, and  $a_{K-W}$  is the radius of the impenetrable core, for the guest-water pairs.



Table A.2: Parameters of the dissociation curves for various single guest clathrate hydrates.  $A$  is dimensionless and  $B$  is in K. Constants for Kr and Xe are given for an Arrhenius law making use of Napierian logarithm.

Molecule	$A$	$B$
N <sub>2</sub>	9.86	-728.58
Ar	9.34	-648.79
Kr	22.3934	-2237.82
Xe	16.62	-3159

Table A.3: Assumed composition of Pluto’s atmosphere at the ground level. Noble gas abundances relative to  $\text{N}_2$  are assumed to be protosolar (Asplund et al. 2009).

Species $K$	Mole fraction $x_K$
$\text{N}_2$	$9.31 \times 10^{-1}$
Ar	$6.92 \times 10^{-2}$
Kr	$4.90 \times 10^{-5}$
Xe	$4.79 \times 10^{-6}$

Table A.4: Relevant parameters of each airglow observation.

Observation	$d_i$ (km)	$t_i$ (s)	$\Omega_i$ ( $\mu$ rad)
PC-Airglow-Fill-0	1116455	6900	3.21
PC-Airglow-Fill-2	819350	600	4.70
PC-Airglow-Fill-2	809012	600	4.77
PC-Airglow-Fill-2	798261	600	4.84
PC-Airglow-Fill-2	788336	600	4.91
PC-Airglow-Fill-2	780204	360	4.97
PC-Airglow-Appr-1a	611833	1200	6.49
PC-Airglow-Appr-1b	575456	600	6.94
PC-Airglow-Appr-2	525813	4200	7.63
PC-Airglow-Appr-3	408242	3600	9.93
PC-Airglow-Appr-4	318118	3000	12.83

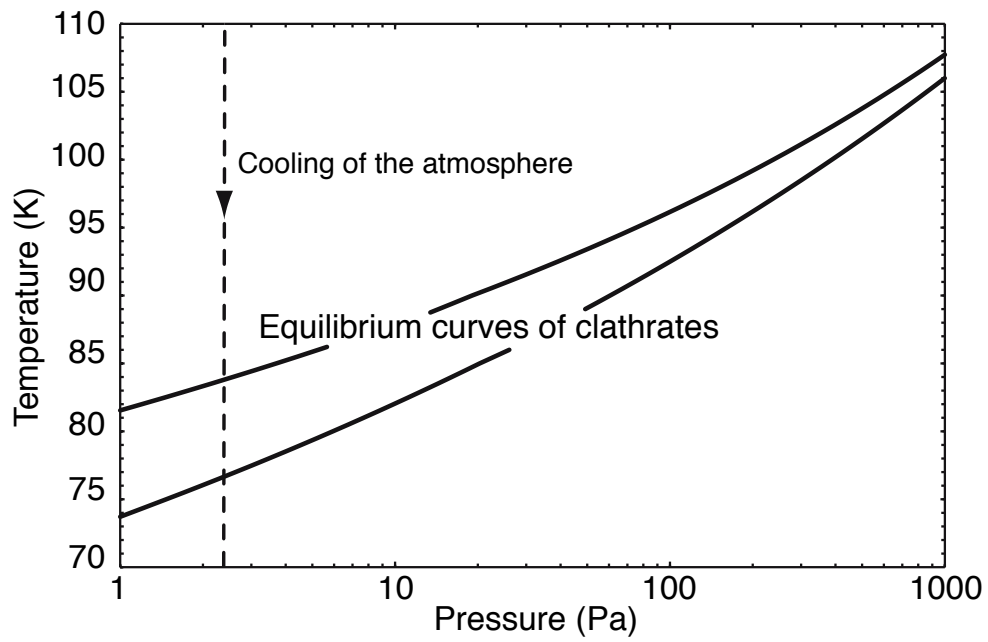


Figure A.1: From top to bottom: equilibrium curves of Xe-, Kr-, and Ar-dominated clathrates (the latter two appear superimposed). The arrow pointing down represents the path followed by a cooling atmosphere with a surface pressure of 2.4 Pa. When the cooling curve intercepts an equilibrium curve, then the corresponding clathrate forms.

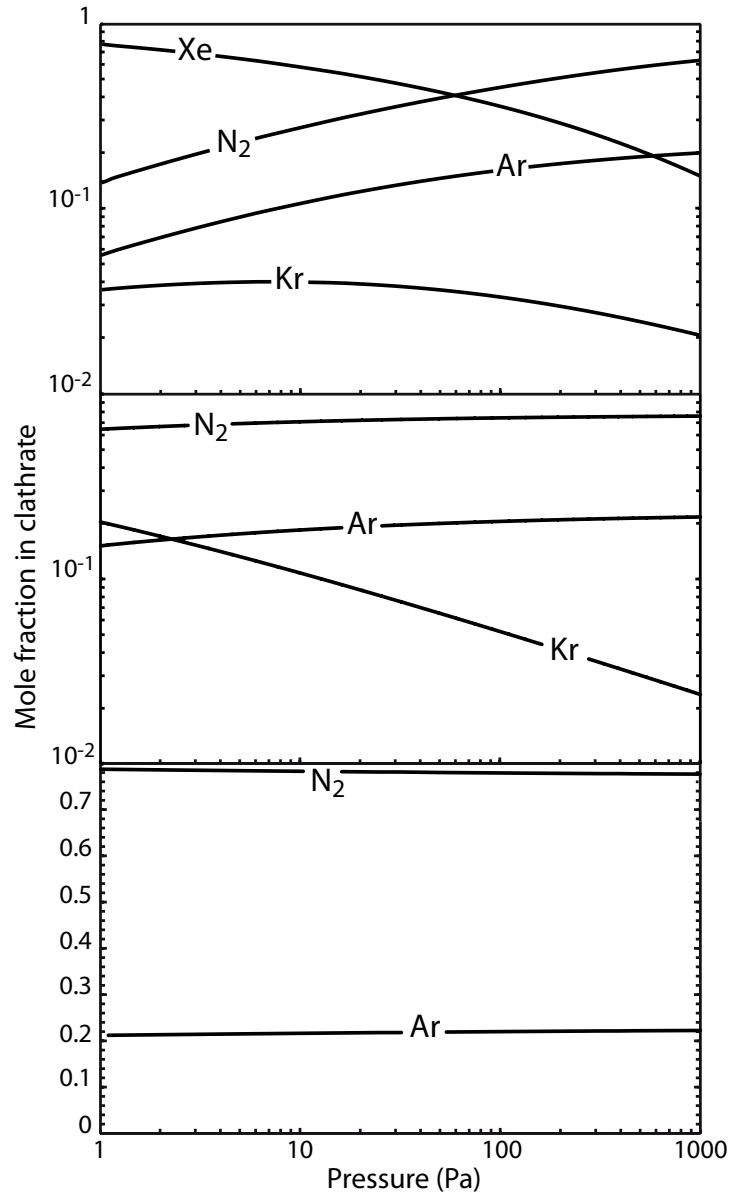


Figure A.2: From top to bottom: mole fractions of volatiles encaged in clathrates that successively form and calculated as a function of the surface pressure of N<sub>2</sub>. Noble gas abundances are assumed to be protosolar relative to N<sub>2</sub> (Asplund et al. 2009). The clathrate composition is investigated from a gas phase composed of Ar, Kr, Xe and N<sub>2</sub> (top panel), of Ar, Kr and N<sub>2</sub> (middle panel), and of Ar and N<sub>2</sub> (bottom panel).

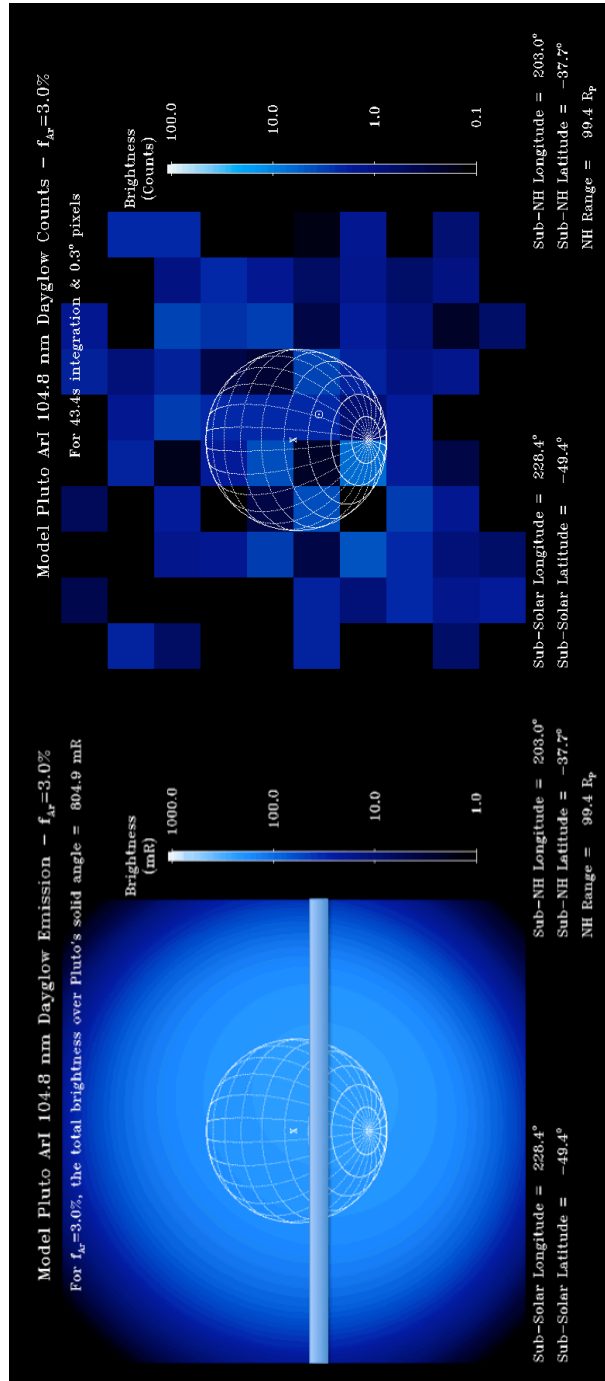


Figure A.3: Left: Simulated Ar I 104.8 nm airglow emission with a 3% mixing ratio.

Right: Count rate images for Alice observation with a 3% mixing ratio.

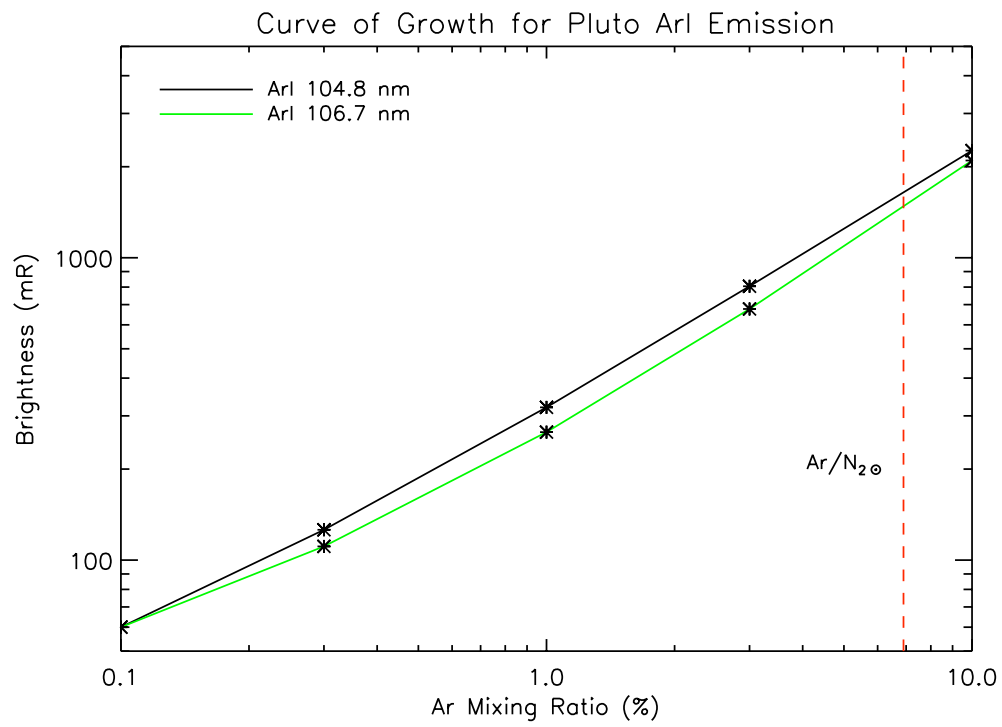


Figure A.4: Emergent Ar I 104.8 and 106.7 nm brightness as a function of mixing ratio.

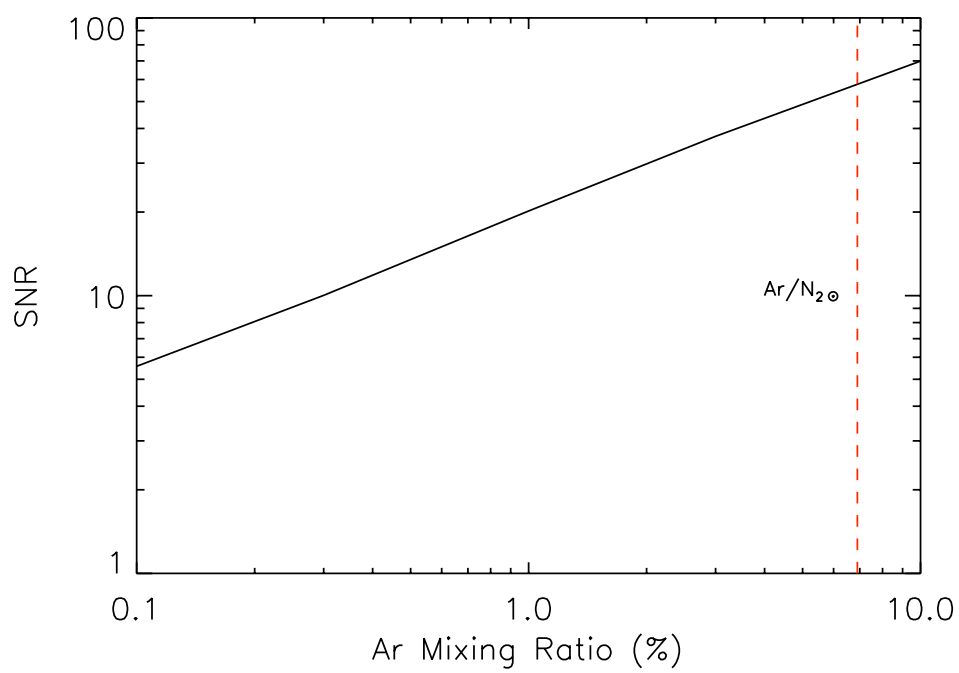


Figure A.5: Signal to noise ratio for the added Ar I 104.8 and 106.7 nm line emission vs. mixing ratio.